

Graph-based Analysis and Optimization of Contention Resolution Diversity Slotted ALOHA

Gianluigi Liva, *Member, IEEE*

Abstract—Contention resolution diversity slotted ALOHA (CRDSA) is a simple but effective improvement of slotted ALOHA. CRDSA relies on MAC bursts repetition and on interference cancellation (IC), achieving a peak throughput $T \simeq 0.55$, whereas for slotted ALOHA $T \simeq 0.37$. In this paper we show that the IC process of CRDSA can be conveniently described by a bipartite graph, establishing a bridge between the IC process and the iterative erasure decoding of graph-based codes. Exploiting this analogy, we show how a high throughput can be achieved by selecting variable burst repetition rates according to given probability distributions, leading to irregular graphs. A framework for the probability distribution optimization is provided. Based on that, we propose a novel scheme, named irregular repetition slotted ALOHA, that can achieve a throughput $T \simeq 0.97$ for large frames and near to $T \simeq 0.8$ in practical implementations, resulting in a gain of $\sim 45\%$ w.r.t. CRDSA. An analysis of the normalized efficiency is introduced, allowing performance comparisons under the constraint of equal average transmission power. Simulation results, including an IC mechanism described in the paper, substantiate the validity of the analysis and confirm the high efficiency of the proposed approach down to a signal-to-noise ratio as low as $E_b/N_0 = 2$ dB.

Index Terms—Bipartite graphs, erasure channel, density evolution, slotted ALOHA, diversity slotted ALOHA, contention resolution diversity slotted ALOHA, successive interference cancellation.

I. INTRODUCTION

WHEREAS the adoption of demand assignment multiple access (DAMA) medium access control (MAC) protocols guarantees an efficient usage of the available bandwidth, random access schemes remain an appealing solution for wireless networks. Among them, slotted ALOHA (SA) [1]–[3] is currently adopted as initial access scheme in satellite communication networks [4], where the large propagation delays make the low access latency of ALOHA-based schemes extremely appealing [5]. Several enhancements of SA have been investigated in the past decades [6]–[8]. Among them, diversity slotted ALOHA (DSA) introduces a burst repetition which, at low normalized loads, yields a slight throughput enhancement respect to SA. A more efficient use of the burst repetition is provided by contention resolution diversity slotted ALOHA (CRDSA) [9].

The intuition behind CRDSA deals with the adoption of interference cancellation (IC) [10]–[13] for resolving collisions.

This paper was presented in part at the International ITG Conference on Source and Channel Coding, Siegen (Germany), Jan. 2010, and in part at the IEEE Global Communications Conference, Miami (US), Nov. 2010.

Gianluigi Liva is with the Institute of Communications and Navigation (Digital Networks Section) of the German Aerospace Centre (DLR), Oberpfaffenhofen, 82234 Weßling, GERMANY (e-mail: Gianluigi.Liva@dlr.de).

More specifically, with respect to DSA, the twin replicas of each burst transmitted within a MAC frame¹ possess a pointer to the slot where the respective copy was sent. Whenever a *clean* burst is detected and successfully decoded, the pointer is extracted and the potential interference contribution caused by the twin replica on the corresponding slot is removed. The procedure is iterated, hopefully permitting the recovery of the whole set of bursts transmitted within the same frame. This results in a remarkably improved throughput T (defined as probability of successful packet transmission per slot) which may reach 0.55, while the peak throughput for pure SA is $T = 1/e \simeq 0.37$. Further improvements may be achieved by exploiting the capture effect [2], [14], especially in presence of power unbalance among different users. CRDSA permits moreover to achieve low packet loss rates (e.g., 10^{-2} or less) at moderate-high loads, whereas SA needs to operate at extremely low loads. Hence for CRDSA most of the burst transmissions are successful at the first attempt, leading to low latencies. CRDSA (as well as the enhancement proposed herein) is currently investigated within the Digital Video Broadcasting (DVB) - Return Channel via Satellite (RCS) standardization as random access scheme for next generation interactive satellite services [15], [16].

In this paper, we propose a novel scheme, referred to as irregular repetition slotted ALOHA (IRSA), which relies on a bipartite graph optimization of CRDSA. In fact, we first show that the iterative burst recovery process can be represented via a bipartite graph. Bipartite graphs have been often used to describe the structure of iteratively-decodable error correcting codes and to analyze their performance under iterative (message-passing) decoding [17]–[20]. Based on the bipartite graph representation of low-density parity-check (LDPC) codes [21], methods for obtaining iterative decoding thresholds close to the Shannon’s limit for many types of communication channels were introduced. The result was achieved by irregular bipartite graph constructions [19], [20], whereas regular graphs usually lead to a loss in terms of iterative decoding threshold. In the CRDSA context, the bipartite graph representation allows analyzing the convergence of the iterative IC process, permitting a fast analytical characterization of the CRDSA performance. We show how the bipartite graph framework can be used to largely improve the performance of CRDSA by allowing a variable repetition rate for each burst, leading to *irregular* graphs (the definitions of *regular* and *irregular* graphs

¹According to [9], in this paper we consider a random access scheme where the slots are grouped into MAC frames. We further restrict to the case where each user proceeds with only one transmission attempt (either related to a new packet or to a retransmission) within a MAC frame.

are provided in Section III). The proposed IRSA scheme is hence based on irregular graphs. The repetition rate is selected by the user according to a probability distribution (which is the object of our optimization), on which the throughput² performance will depend. Extensions of the proposed analysis accounting for possible impairments and capture effects are outlined in Appendix A. The simulation results, including an actual IC technique described in Appendix B, confirm the validity of the proposed analytical tools, which permit an accurate prediction of the throughput for large frames. It is further shown that, even under the assumption of small MAC frames, the proposed technique still achieves a high throughput. Large performance gains are also demonstrated in terms of packet loss rates.

The remainder of this paper is organized as follows. In Section II an overview of the system is provided. The graph representation is discussed in Section III, while the iterative IC analysis is presented in Section IV. An analysis in terms of normalized efficiency is provided in Section V, allowing performance comparisons under the assumption of equal average transmission power. Numerical results on the throughput and the packet loss rate of IRSA are presented in Section VI. The conclusions follow in Section VII.

II. SYSTEM OVERVIEW

We will consider next MAC frames of duration T_F , each composed of n slots of duration $T_S = T_F/n$. The transmission of a packet (or burst)³ is enforced within one slot. We will assume that in each MAC frame a finite number (m) of users attempts a packet transmission. Without losing generality, each of the m users performs a single transmission within each MAC frame, either related to a new packet or to the retransmission of a collided one. Furthermore, retransmissions shall not take place within the same MAC frame where the collision happened. Hence, among the m users, some may be back-logged. The normalized offered traffic (or channel traffic) G is given by $G = m/n$, and represents the average number of packet transmissions per slot. The normalized throughput (or channel output) T is defined as the probability of successful packet transmission per slot. In a framed SA case (Fig. 1a), each packet is transmitted once in a MAC frame, and eventual collisions lead to retransmissions in the following frames. For SA, the throughput can be expressed as a function of G as $T(G) = Ge^{-G}$. The peak throughput $T = 1/e \simeq 0.37$ is achieved at $G = 1$.

CRDSA relies on the repetition of each burst within the same MAC frame. In each burst replica, a pointer to the position of the twin burst is included, e.g. in a dedicated header field. Whenever a *clean* burst (i.e., a burst which did not collide) is successfully decoded, the pointer is used to determine the slot where the twin burst has been transmitted. Supposing that the burst replica has collided, it is possible to subtract, from the signal received in the corresponding

²The analysis presented in this paper focuses on the throughput/packet loss rate performance. A thorough analysis on other performance metrics (e.g. delay, stability) as in [22] is not considered here.

³The notation *burst* and *packet* will be interchangeably used to denote layer-2 data units.

slot, the interference contribution of the twin packet. This may allow the decoding of another burst transmitted in the same slot. The IC proceeds iteratively, i.e., *cleaned* bursts may allow solving other collisions. CRDSA brings to a remarkable throughput improvement w.r.t. SA over a wide range of loads. Furthermore, the limit for which the throughput is almost linear in G is extended from 0.1 for SA to 0.4 for CRDSA.⁴ This means that for loads lower than 0.4, the burst loss probability is kept remarkably low [9].

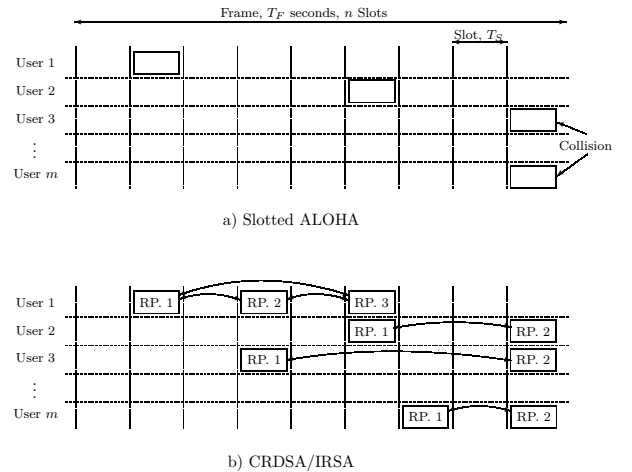


Fig. 1. Overview of the slotted ALOHA (a) and the CRDSA/IRSA (b) protocols (framed). The frame is made by n slots and lasts T_F seconds. The number of users attempting a transmission is m . In the CRDSA/IRSA case (b), a burst is repeated within the MAC frame d times (where d is fixed for CRDSA, while it may vary among users in the IRSA case). Each burst contains a header with a pointer to the position of its replicas. Whenever a burst is successfully received, the pointer is extracted, and the replica positions are identified. The interference contribution caused by the replicas can be then removed, i.e. the signal waveform associated with the burst is reconstructed, and it is subtracted from the signal received in the slots where the replicas have been transmitted. In the example above, a replica of the burst transmitted by User 1 is received without collisions (second slot from the left). Its contribution on the 4th and the 6th slots can be removed. In the 4th and in the 6th slots, the bursts transmitted by Users 3 and 2 can be decoded. The process proceeds iteratively.

The approach proposed in this paper is a generalization of the above-described one. When IRSA is used, each burst is transmitted l times within the MAC frame, where the repetition rate l varies from burst to burst (Fig. 1b) according to a given probability distribution. CRDSA can be seen as a special case of IRSA, where the repetition rate is fixed to $l = 2$.⁵

⁴For CRDSA/IRSA the relation $G = m/n$ still holds, i.e. G still relates to the number m of transmission attempts (it is not influenced by the number of replicas). Thus a packet replicated l times counts as 1 transmission attempt. Hence, G represents in a certain sense the *logical* load of the channel, in contrast with the *physical* load, which for CRDSA is $2G$. Note that the physical load represents the average number of burst replicas that are transmitted per slot, and therefore it does not provide a direct measure of the traffic handled by the scheme, which is in fact given by the logical load.

⁵Through this paper, we will refer to CRDSA as it in original definition [9], i.e. with constant repetition rate $l = 2$. Recently, CRDSA has been extended in a way that each burst can be repeated more than 2 times [14]. However, also in that case the repetition rate l is constant and a-priori fixed for all the bursts. The performance of CRDSA with $l > 2$ repetitions will be considered in Sections IV-B and VI.

III. GRAPH REPRESENTATION OF THE IC PROCESS

The IRSA approach works as follows: for each transmission, the user adopts a variable repetition rate, which is picked according to a given distribution $\{\Lambda_d\}$ (see Fig. 1b), i.e. for a generic packet l replicas are transmitted within the MAC frame with a probability Λ_l .

It is now convenient to introduce a graph representation of the IC process. We keep on considering a MAC frame composed of n slots, in which m users attempt a transmission. The frame status can be described by a bipartite graph, $\mathcal{G} = (B, S, E)$, consisting of a set B of m *burst nodes* (one for each burst that is transmitted), a set S of n *sum nodes* (one for each slot in the frame), and a set E of edges. An edge connects a burst node (BN) $b_i \in B$ to a sum node (SN) $s_j \in S$ if and only if a replica of the i -th burst is transmitted in the j -th slot. Loosely speaking, BNs correspond to bursts and SNs correspond to slots. Similarly, each edge corresponds to a burst replica. Hence, a burst with l replicas is represented by a BN with l neighbors (i.e. a BN from which l edges emanate). A slot where l replicas collide corresponds to a SN with l connections. As an example, the bipartite graph describing a frame made by $n = 4$ slots where $m = 4$ transmission attempts take place is depicted in Fig. 2a, where squares denote SNs, and circles denote BNs. The number of edges connected to a node is referred to as the *node degree*. Graphs for which the BN degree is constant will be referred to as *regular* graphs. In contrast, graphs for which the BN degree varies from BN to BN will be referred to as *irregular* graphs. It follows that CRDSA leads to regular graphs, while IRSA allows irregular graphs. The IC process can be represented through a message-passing along the edges of the graph. More specifically, assuming the case where no capture effect is exploited, a burst replica can be revealed by two means, i.e.

- The burst replica has been successfully decoded in the slot where it has been sent. This is possible if the interference caused by other burst replicas (colliding in the same slot) has been removed, or if no collisions at all happened in the slot.
- The corresponding burst has been recovered elsewhere.

Example. An example of a graph representation is provided in Fig. 2. We label each edge with a ‘1’ if the corresponding burst replica has been revealed. Otherwise, the edge is labeled as ‘0’. The iterative IC process starts (b) by decoding the second burst (the burst is received without collisions within the second slot, in fact the degree of the second SN is 1). The contribution of the second burst can be removed from the slots where its replicas were transmitted. The revealed edges (labeled as ‘1’) are then removed from the graph. During the second iteration (c), we look for SNs with residual degree 1. Those nodes represent the slots where, after the first IC iteration, cleaned bursts can be now detected. The only degree-1 SN in (c) is the first one, from which it is possible to recover the first burst. Its contribution into the third slot is then removed (d). During the third iteration, B_3 is recovered. Accordingly, the edge connecting B_3 to S_4 is revealed. The contribution of the third burst into the fourth slot is cancelled, allowing the recovery of the fourth burst (e).

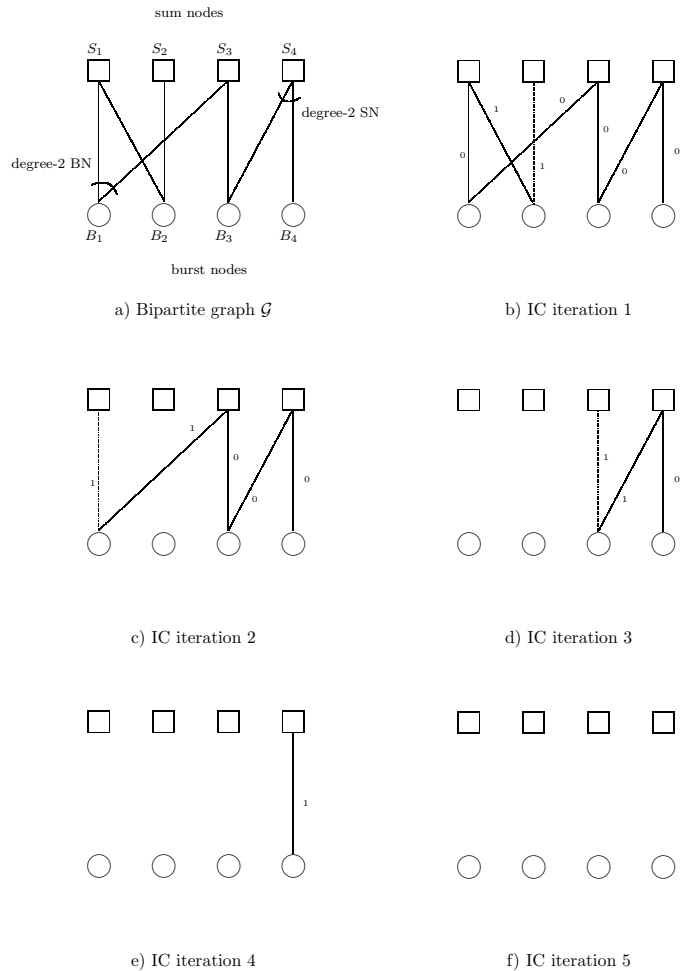


Fig. 2. Graph representation of the IC iterative process.

A. Node- and Edge-Perspective Degree Distributions

We introduce next the concept of *node-perspective degree distribution*. The burst node degree distribution is defined by $\{\Lambda_l\}$, where Λ_l denotes the probability that a BN possesses l connections. The SN degree distribution is represented by $\{\Psi_l\}$, where Ψ_l is the probability that a SN possesses l connections.⁶ Polynomial representations of the node-perspective degree distributions are given by

$$\Lambda(x) \triangleq \sum_l \Lambda_l x^l, \quad \Psi(x) \triangleq \sum_l \Psi_l x^l.$$

The BN degree distribution $\Lambda(x)$ is under full control of the system designer. This is indeed not the case for the SN degree distribution $\Psi(x)$. It will be shown that the SN degree distribution is fully defined by the system load G and by the average burst repetition rate. The average burst repetition rate is given by $\sum_l l \Lambda_l = \Lambda'(1)$, while the average number of collisions per slot is $\sum_l l \Psi_l = \Psi'(1)$.⁷ It is easy to verify that $G = m/n = \Psi'(1)/\Lambda'(1)$.

⁶Consistently with the definition at the beginning of Section III, Λ_l is also the probability that a burst is replicated l times. Ψ_l represents instead the probability that l bursts replicas would be transmitted within a given slot.

⁷We denote by $f'(x) = df(x)/dx$. Hence $\Lambda'(x) = \sum_l l \Lambda_l x^{l-1}$ and $\Psi'(x) = \sum_l l \Psi_l x^{l-1}$.

Degree distributions can be defined also from an *edge perspective*. We define λ_l as the probability that an edge is connected to a degree- l BN. Similarly, ρ_l defines the probability that an edge is connected to a SN of degree l . It follows from the definitions that

$$\lambda_l = \frac{\Lambda_l l}{\sum_l \Lambda_l l}, \quad \rho_l = \frac{\Psi_l l}{\sum_l \Psi_l l}.$$

The polynomial representations of $\{\lambda_l\}$ and $\{\rho_l\}$ are⁸

$$\lambda(x) \triangleq \sum_l \lambda_l x^{l-1}, \quad \rho(x) \triangleq \sum_l \rho_l x^{l-1}.$$

The relations $\lambda(x) = \Lambda'(x)/\Lambda'(1)$ and $\rho(x) = \Psi'(x)/\Psi'(1)$ follow from the definitions above.

IV. ITERATIVE IC CONVERGENCE ANALYSIS

Consider now a degree- l BN. Denote by q the probability that an edge is unknown, given that each of the other $l-1$ edges has been revealed with probability $1-p$ during the previous iteration step. The edge is revealed whenever at least one of the other edges have been revealed. Hence, $q = p^{l-1}$. In a similar manner, consider a SN with degree l . According to the notation introduced so far, p denotes the probability that an edge is unknown, given that each of the other $l-1$ edges have been revealed with probability $1-q$ in the previous iteration step. The edge is revealed whenever all the other edges have been revealed. Hence, $1-p = (1-q)^{l-1}$ or equivalently $p = 1 - (1-q)^{l-1}$.⁹ According to the tree analysis argument of [18], by averaging these two expressions over the edge distributions, one can derive the evolution of the average erasure probabilities during the i -th iteration as

$$q_i = \sum_l \lambda_l p_{i-1}^{l-1} = \lambda(p_{i-1}) \quad (1)$$

and

$$p_i = \sum_l \rho_l \left(1 - (1 - q_i)^{l-1}\right) = 1 - \rho(1 - q_i), \quad (2)$$

where the subscript i denotes the iteration number that, for the sake of simplicity, will be omitted in the rest of the paper. By iterating (1),(2) for a given amount of times (I_{max}), it is possible to analyze the convergence of the IC process.¹⁰ The initial condition has to be set as $q_0 = p_0 = 1$ (there are no revealed edges at the beginning of the process). Following (2), at the first iteration p is the probability that an edge is not connected to any degree-1 SN.

Note that the recursion of (1),(2) holds if the messages exchanged along the edges of the graph are statistically

⁸For the node-perspective degree distributions we associate the coefficients (Λ_l, Ψ_l) to x^l . In the edge-perspective case the coefficients (λ_l, ρ_l) are related to the x^{l-1} term. This choice will bring to a compact description of the IC process.

⁹Similar equations were developed in [9, Sec.III.D] for deriving an upper bound to the throughput of CRDSA.

¹⁰This approach is in fact equivalent to the density evolution analysis for LDPC codes [20]. However, note that the IC process of IRSA and the erasure recovery process of LDPC codes are similar, but not strictly the same. In fact, while for IRSA the entire graph is active in the collision resolution, in the LDPC codes case just the sub-graph induced by the erasure pattern is involved in the erasure recovery process.

independent. Thus, the accuracy of (1),(2) is subject to the absence of loops in the graph (recall that loops introduce correlation in the evolution of the erasure probabilities). This assumption implies very large frame sizes ($n \rightarrow \infty$), hence the analysis presented next will refer to this asymptotic setting. It is crucial to remark that this hypothesis is nevertheless needed just in the system design phase for deriving a simple $\Lambda(x)$ distribution optimization criterion. We will see that this criterion remains valid also for short or moderate-length frames. In particular, it will be shown by numerical results that probability distributions designed for the asymptotic setting turn to be effective also for realistic frame sizes.

By fixing $\Lambda(x)$ (and hence $\lambda(x)$), for each value of the offered traffic G the distribution $\rho(x)$ can be determined. For values of G below a certain threshold G^* , the bursts will be recovered with a probability close to 1. Above the threshold G^* , the procedure will fail with a probability bounded away from 0. Hence, we define the threshold G^* as the maximum value of G such that

$$q > \lambda(1 - \rho(1 - q)), \quad \forall q \in (0, 1]. \quad (3)$$

We will look for distributions $\Lambda(x)$ leading to a high threshold G^* , allowing (in the asymptotic setting) transmission with vanishing error probability for any offered traffic up to G^* .

A. Derivation of the Sum Nodes Distribution

To get the threshold for a given $\Lambda(x)$ we have first to derive $\rho(x)$. Recalling that the average number of collisions per burst is $\Psi'(1)$ and that m users attempt a transmission in a MAC frame, the probability that a generic user sends a burst replica within a given slot is $\Psi'(1)/m$. Thus, the probability that a SN has degree l is given by

$$\Psi_l = \binom{m}{l} \left(\frac{\Psi'(1)}{m}\right)^l \left(1 - \frac{\Psi'(1)}{m}\right)^{m-l}.$$

The node-perspective SNs degree distribution results in

$$\Psi(x) = \sum_l \Psi_l x^l = \left(1 - \frac{\Psi'(1)}{m}(1-x)\right)^m. \quad (4)$$

By letting $m \rightarrow \infty$ (asymptotic setting), (4) becomes $\Psi(x) = \exp(-\Psi'(1)(1-x)) = \exp(-G\Lambda'(1)(1-x))$.¹¹ Recalling the identities provided at the end of Section III, the polynomial representation of the edge-perspective SNs distribution is obtained as

$$\rho(x) = \frac{\Psi'(x)}{\Psi'(1)} = e^{-G\Lambda'(1)(1-x)}. \quad (5)$$

By replacing (5) in (3), the threshold G^* is defined as the maximum value of G such that

$$q > \lambda\left(1 - e^{-qG\Lambda'(1)}\right), \quad \forall q \in (0, 1]. \quad (6)$$

¹¹For large n the number of transmissions in a slot follows a Poisson distribution, $\Psi_l = (1/l!)(G\Lambda'(1))^l \exp(-G\Lambda'(1))$. As pointed out by one of the anonymous reviewers, the graph representation for IRSA is closely related to that of Luby-Transform (LT) codes [23]. For LT codes, the *encoding symbol degrees* (corresponding to the SNs degrees of the IRSA case) are defined by the code designer, whereas *input symbols* (which correspond to BNs) involved in an equation are selected with a uniform distribution, resulting for large blocks in Poisson-distributed input symbol degrees.

Define now $f(q) \triangleq \lambda(1 - \exp(-qG\Lambda'(1)))$. A simple upper bound on the threshold can be obtained by observing that, for $q \rightarrow 0$ and for $G \leq G^*$, the derivative of $f(q)$ with respect to q must be less or equal than one, i.e. $f'(0) \leq 1$. This turns in $\lambda'(0)\Lambda'(1)G = \lambda_2\Lambda'(1)G \leq 1$ and hence in the bound on the threshold is given by

$$G^* \leq \frac{1}{\lambda_2\Lambda'(1)}. \quad (7)$$

In the IRSA case, this bound is the counterpart of a similar bound (referred to as *stability condition*) on the decoding threshold for LDPC codes over the erasure channel [20].

B. Examples of Degree Distributions

Examples of distributions are provided next. We refer to those with constant repetition rate l as *l-regular distributions*. The others will be referred to as *irregular distributions*.

Example 1 (Slotted ALOHA). The SA can be considered as a 1-regular distribution with $\Lambda_1(x) = x$. No threshold can be derived since no iterative IC process can take place. Note that the throughput SA relates to the fraction of slots where one and only one transmission attempt has been performed. Such a fraction is given by the coefficient of the degree-1 term of $\Psi(x)$. Taking the Taylor's expansion of (5) around $x_0 = 0$, the coefficient of the degree-1 term is given by $G\Lambda'(1)e^{-G\Lambda'(1)}$, where $\Lambda'(1) = 1$. Thus, $T = Ge^{-G}$.

Example 2 (CRDSA). The approach of [9] leads to a 2-regular distribution (i.e., $\Lambda_2(x) = x^2$). The threshold derived according to (6) is $G^* = 0.5$. In this specific case, the actual threshold matches with equality the condition (7).

Example 3 (IRSA with distribution $\Lambda_3(x)$). The distribution optimization has been obtained by differential evolution [24]. The maximum degree has been fixed to 8 due to practical considerations, i.e. to limit the number of pointers in the burst header.¹² The distribution is given by $\Lambda_3(x) = 0.5x^2 + 0.28x^3 + 0.22x^8$, and the corresponding threshold is $G^* = 0.938$. The evolution iteration after iteration of the probability q , according to the equation $q_{i+1} = \lambda(1 - \exp(-q_iG\Lambda'(1)))$ obtained by combining (1), (2) and (5), is presented in Fig. 3.

In Figure 4, the asymptotic ($n \rightarrow \infty$) performance for the three distributions is presented in terms of MAC burst loss probability, P_L (i.e., the probability that a transmission attempt does not succeed) vs. the normalized offered traffic. The relation between throughput and burst loss probability is given by $T(G) = G(1 - P_L(G))$. The burst loss probability has been obtained by iterating (for each value of G) equations (1) and (2) for a maximum of $I_{max} = 1000$ times, and by finally setting $P_L = \Lambda(p)$.¹³ The gain achievable by adopting

¹²In practical implementations, the overhead due to the inclusion of pointers in the header of the burst may be reduced by adopting more efficient techniques. One may include in the header the repetition degree for the burst together with a random seed, out of which it is possible to reconstruct (by a pre-defined pseudo-random number generator) the positions of the burst replicas.

¹³In fact, the probability that a burst is lost after a certain amount of iterations is given by the probability that all the edges connected to the corresponding BN are unrevealed. Assuming a node with l connections, such probability is p^l . By averaging on the BNs distribution, we get $P_L = \sum_l \Lambda_l p^l = \Lambda(p)$.

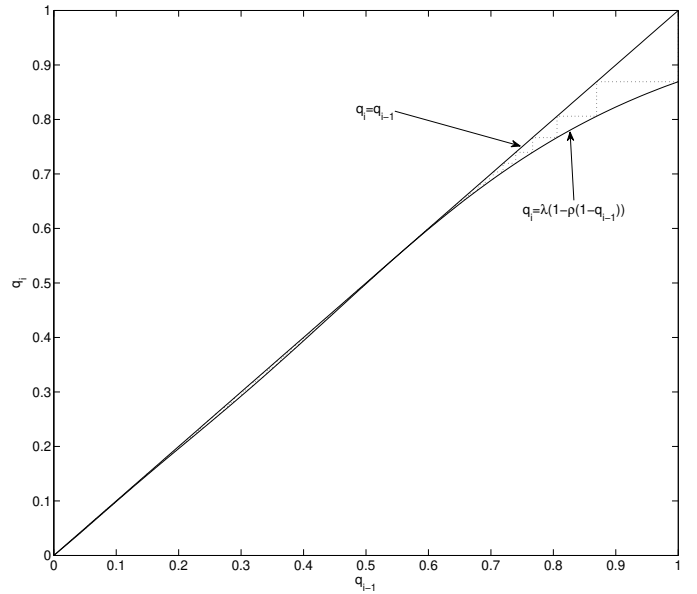


Fig. 3. Evolution of the probability q for the case of $\Lambda_3(x)$ according to the equation $q_{i+1} = \lambda(1 - \exp(-q_i G\Lambda'(1)))$, when operating at the threshold, i.e. with $G = G^* = 0.938$.

the irregular distribution $\Lambda_3(x)$ is evident in this asymptotic setting. According to the threshold definition, all the offered traffic for $G \leq G^* = 0.938$ turns in useful throughput (i.e., the burst loss probability is essentially 0). For the approach of [9], this holds just for $G \leq 0.5$. Simulation results for short frames and a reasonable number of iterations, presented in Section VI, will confirm the validity of the proposed asymptotic optimization criterion.

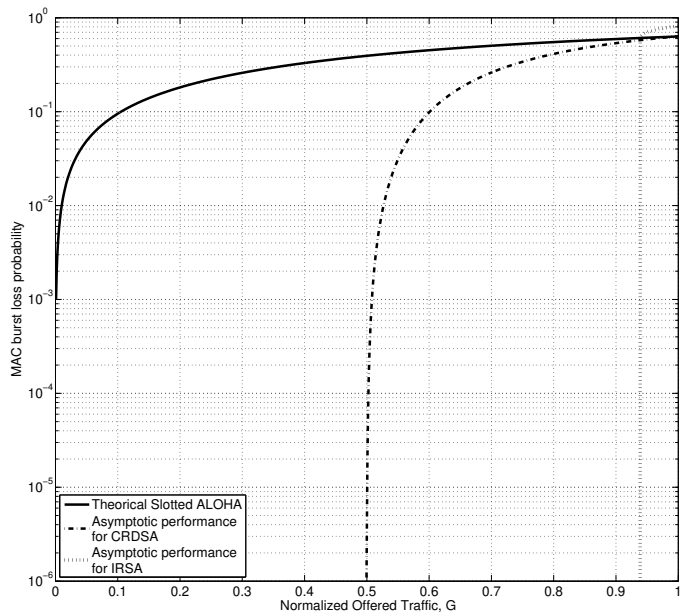


Fig. 4. Asymptotic performance in terms of MAC packet (burst) loss probability, P_L , vs. offered traffic, G , for SA, CRDSA, and for IRSA with the irregular distribution $\Lambda_3(x) = 0.5x^2 + 0.28x^3 + 0.22x^8$.

In Table I, degree distributions (obtained by differential evolution [24]) for different maximum repetition rates are pre-

sented. The use of repetition rates higher than 8 allows achieving thresholds close to 1. With a maximum repetition rate to 16, it is possible to get $G^* = 0.965$. Even when the maximum repetition rate is limited to a low value, large threshold values are achieved. To say, with a maximum repetition rate 4, a threshold $G^* = 0.868$ is reached. For the sake of comparison, we computed the threshold of a 4-regular distribution, i.e. a distribution with constant repetition rate 4 [14], which is $G^* = 0.772$. Thus, asymptotically the irregular distribution with maximum repetition rate equal to 4 permits to enhance the throughput of roughly 12% w.r.t. the 4-regular CRDSA case. Similarly, the optimized distribution with maximum repetition rate 5 reaches a threshold $G^* = 0.898$, while for the 5-regular CRDSA case [14] the threshold is $G^* = 0.701$. In this case, the throughput gain is nearly 28%.

TABLE I
THRESHOLDS COMPUTED FOR DIFFERENT DISTRIBUTIONS

Distribution, $\Lambda(x)$	G^*
$0.5102x^2 + 0.4898x^4$	0.868
$0.5631x^2 + 0.0436x^3 + 0.3933x^5$	0.898
$0.5465x^2 + 0.1623x^3 + 0.2912x^6$	0.915
$0.5x^2 + 0.28x^3 + 0.22x^8$	0.938
$0.4977x^2 + 0.2207x^3 + 0.0381x^4 + 0.0756x^5 + 0.0398x^6 + 0.0009x^7 + 0.0088x^8 + 0.0068x^9 + 0.0030x^{11} + 0.0429x^{14} + 0.0081x^{15} + 0.0576x^{16}$	0.965

V. REMARKS ON THE NORMALIZED EFFICIENCY

The comparisons carried out so far assume the same physical layer configuration (i.e., modulation and coding) and the same peak transmitting power for all the analyzed schemes (SA, CRDSA, IRSA). This assumption is correct for many concrete applications, where the peak power available for the terminal transmissions is bounded by practical reasons (e.g. performance of the amplifiers and/or by regulations on the spectrum usage). In this condition, the choice of the modulation/coding scheme used for protecting each burst is tailored to the signal-to-noise ratio (SNR) with which the bursts are received. Hence, SA, CRDSA and IRSA would transmit with the same spectral efficiency, and the throughput comparison among the different schemes reflects the actual amount of information that is conveyed by them.

It is nevertheless clear that CRDSA/IRSA require on average more power than SA. This is due to the average number of packet repetitions required by the schemes, which is (by neglecting the retransmissions due to unresolvable collisions) 1 for SA, 2 for CRDSA (as in its original setting [9]) and in general $\Lambda'(1)$ for IRSA. Following the approach proposed in [3], one can compute the efficiency of a MAC scheme normalized to the capacity of the multiple access Gaussian channel under the constraint on the overall received signal power (*normalized efficiency*). Given the average aggregate signal power P ($P = \sum_{i=1}^m P_i$ with P_i being the average power for the i -th terminal) and the noise power N ,

the sum-rate multiple access channel capacity is given by $C_{ref} = \log(1 + P/N)$ [25]. Following [3], for a generic ALOHA-based access scheme the capacity can be evaluated as $C_i = T_i(G) \log(1 + P/(ND))$, where D denotes the ratio between the average transmitted power and the power used for the transmission of a burst (replica). For SA, $D = G$ and $C_1 = Ge^{-G} \log(1 + P/(NG))$. For CRDSA, $D = 2G$ and hence $C_2 = T_2(G) \log(1 + P/(2NG))$, while for IRSA, $D = \Lambda'(1)G$ and $C_3 = T_3(G) \log(1 + P/(\Lambda'(1)NG))$, where $T_2(G)$ and $T_3(G)$ are the throughput vs. offered traffic functions of CRDSA and IRSA, for which a closed-form expression is not available. By fixing the overall received signal power, and hence the signal to noise ratio $P/N = E_s/N_0$, it is possible to compare the efficiency of the schemes w.r.t. the channel capacity limit in terms of normalized efficiency as $\tilde{\eta}_i = C_i/C_{ref}$.

VI. NUMERICAL RESULTS

Simulation results are presented next. The simulations have been carried out at two levels. A first type of simulations deals with the MAC layer only. In this case, we considered that a burst is recovered if and only if there is no interference contribution in the corresponding slot (i.e., no collision happened or the contributions of all the colliding bursts have been cancelled). A second type of simulations included a complete implementation of the signal waveform received at the burst demodulator (comprising, apart from the Gaussian noise, random phase/frequency/timing offsets) and of the physical layer receiver algorithms. In this case, an actual IC mechanism has been used (details in the Appendix B) and complemented by the forward error correcting scheme included in the last version of the DVB-RCS standard [4], [26]. A comparison between the results obtained by the two approaches is presented, which shows that the first (MAC layer) approach, despite of its simplicity, tightly matches the results obtained through a complete simulation of the physical layer algorithms (which is indeed much more complex), at least down to moderate-low packet loss rates.¹⁴ In the following, unless otherwise stated, by “simulations” we will denote MAC layer simulations. No capture effect, which may lead to throughput gains, is considered. For IRSA, we adopted the distribution $\Lambda_3(x)$ introduced in Section IV-B.

A first set of simulations assumes a fixed frame size of $n = 200$ slots, which is considered among the typical values for CRDSA and IRSA in interactive satellite systems [9]. Recall that the number of users attempting a transmission within the frame is given by $m = Gn$. In Fig. 5, the reference throughput curve for SA and the asymptotic curves (obtained by the iterative IC analysis) for CRDSA and IRSA are provided for $G \in [0, 1]$. Focusing on the simulation results, with $I_{max} = 100$ iterations, IRSA achieves a throughput close to 0.8, while CRDSA does not exceed $T = 0.55$. By limiting the iteration count to 10 (a case of interest for low-complexity implementations [9]), IRSA shows a small throughput degradation with respect to the case of $I_{max} = 100$. The relation

¹⁴Similarly, the analysis provided in [9, Sec.V] showed that the performance obtained by MAC layer simulations is very close to that achieved by simulating the entire IC process, down to $E_s/N_0 = 5$ dB.

throughput vs. load is linear almost up $T = 0.7$. Up to such values, most of the traffic turns into throughput. The behavior of IRSA when G approaches 1 deserves further comments. While for values of G that are quite below the threshold G^* the advantage of CRDSA and IRSA with respect to SA is evident, at higher traffic values SA outperforms the contention resolution schemes. This is due to the threshold phenomenon related to the iterative IC process. For $G < G^*$ the iterative burst recovery works well and most of the collisions are resolved. As $G > G^*$, the IC process gets stuck in an early stage, when number of burst replicas (i.e. the physical load) within the frame is much larger than the number of bursts of a SA scheme, resulting in a high packet loss rates.

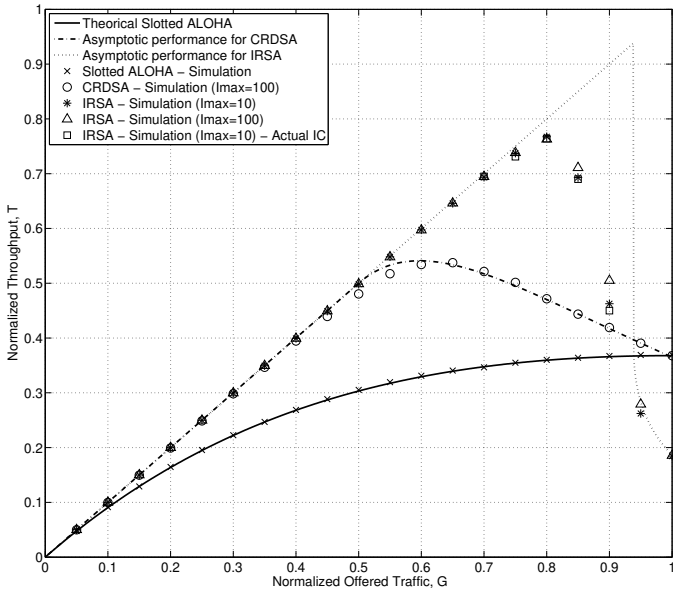


Fig. 5. Simulated and asymptotic throughput for SA, CRDSA, and for IRSA with $\Lambda_3(x) = 0.5x^2 + 0.28x^3 + 0.22x^8$. $n = 200$. The results obtained by simulating the actual IC mechanism (specified in the Appendix B) are denoted by the marker '□', and are referred to a SNR at $E_b/N_0 = 2$ dB.

Note that for the IRSA case the peak throughput with a frame of $n = 200$ slots is lower than that predicted by the iterative IC analysis. It is however reasonable that the asymptotic performance shall be approached by considering larger frames. The results in Fig. 6 confirm this fact. Here, the performance of IRSA are depicted, assuming 20 iterations, for different frame sizes $n = 50, 200, 1000$. The chart shows that the scheme benefits from adopting longer MAC frames. For CRDSA the phenomenon is less visible, and already with $n = 200$ the gap from the asymptotic prediction is negligible.

In Fig. 7 the packet loss rates (PLRs) for SA and different CRDSA/IRSA schemes are compared. The simulations were performed for frames with $n = 200$ slots and with $I_{max} = 20$ iterations. Targeting a $PLR = 10^{-2}$, one can note how SA would need to operate at low loads ($G \simeq 0.01$), while as already observed in [9] CRDSA with two repetitions would be able to sustain a traffic close to $G \simeq 0.35$. The IRSA scheme based on the $\Lambda_3(x)$ distribution is able to double the load w.r.t. to CRDSA for the same target PLR. In fact a $PLR = 10^{-2}$ is achieved at a channel traffic $G \simeq 0.7$. The IRSA scheme

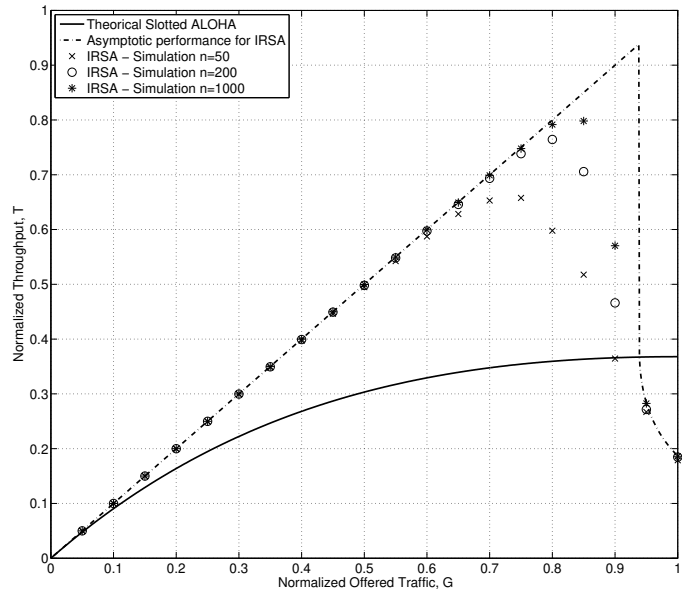


Fig. 6. Simulated and asymptotic throughput for SA and IRSA with $\Lambda_3(x) = 0.5x^2 + 0.28x^3 + 0.22x^8$. Various MAC frame sizes. $I_{max} = 20$.

tends to show a flooring effect at low offered traffic regimes. More specifically, the PLR curve shows a remarkable loss in the steepness just below $PLR = 10^{-2}$, i.e. for $G < 0.7$. Interestingly, also the CRDSA scheme with only 2 repetitions suffers for a lack of steepness in its PLR performance curve. As already observed in [14], the adoption of a CRDSA scheme with a larger regular repetition brings to lower error floors. The result for a 4-regular CRDSA is also provided in Fig. 7. Remarkably, the floor disappears, at least down to $PLR \simeq 10^{-4}$, while a performance loss of the 4-regular CRDSA scheme can be observed w.r.t. the $\Lambda_3(x)$ -based IRSA case at moderate-high PLRs. In fact a $PLR = 10^{-1}$ is achieved with $G \simeq 0.72$ for the 4-regular CRDSA, while IRSA allows achieving that loss rate at $G \simeq 0.83$. The high error floors of the $\Lambda_3(x)$ -based IRSA scheme and the poor PLR performance of the 2-regular CRDSA can be related to specific combinations of collisions which block the iterative IC process. In terms of graph representations, such collision patterns are inherently related to (short) cycles in the bipartite graph, leading to so-called *stopping sets*. In the LDPC codes context, a *stopping set* is any set of variable nodes such that any check node connected to this set is connected to it at least twice [27]. In analogy to that, in the CRDSA/IRSA context we shall re-define a stopping set as any set of BNs such that any SN connected to this set is connected to it at least twice. Assuming that no capture effect is adopted, it follows that such graph configurations lead to unresolvable burst collisions. In the case of LDPC codes for erasure correction, it is well known that the impact of small stopping sets in the finite-length code performance is strictly related to the fraction of degree-2 variable nodes in its bipartite graph [28], [29]. We conjecture that in the CRDSA/IRSA case a similar role is played by degree-2 BNs. This conjecture is strengthened by the observation that the distribution $\Lambda_3(x)$ is based on a large fraction (0.5) of degree-2 BNs, while in the 2-regular CRDSA case the totality of the BNs possesses

a degree 2. We designed hence a new BN distribution, in which we limited the fraction of degree-2 burst nodes to 0.25. The resulting distribution is denoted by $\Lambda_4(x)$ and is given by $\Lambda_4(x) = 0.25x^2 + 0.60x^3 + 0.15x^8$. The corresponding threshold is $G^* = 0.892$, slightly less than that of $\Lambda_3(x)$. The simulation results provided in Fig. 7 confirm that the limitation of degree-2 BNs allows reducing the error floor, which is lowered w.r.t. the $\Lambda_3(x)$ case by nearly one order of magnitude. Indeed, if the PLR is used as a metric for selecting the BN distribution, a different choice of the distribution shall be applied depending on the target loss rate. To say, when the target is $\text{PLR} \simeq 10^{-2}$ or $\text{PLR} \simeq 10^{-3}$, the distribution $\Lambda_4(x)$ shall be used. When the PLR requirement is relaxed to $\text{PLR} \simeq 10^{-1}$, $\Lambda_3(x)$ represents the best choice. When there is a demand for very low PLRs, the best choice could be a 4-regular CRDSA. These considerations hold for the frame size considered in this example (i.e., $n = 200$ slots), and may change for different frame sizes. For very large frames the error floors would be much lower, and the asymptotic results of Fig. 4 could be considered as a first estimation of the actual PLR performance of the different schemes.

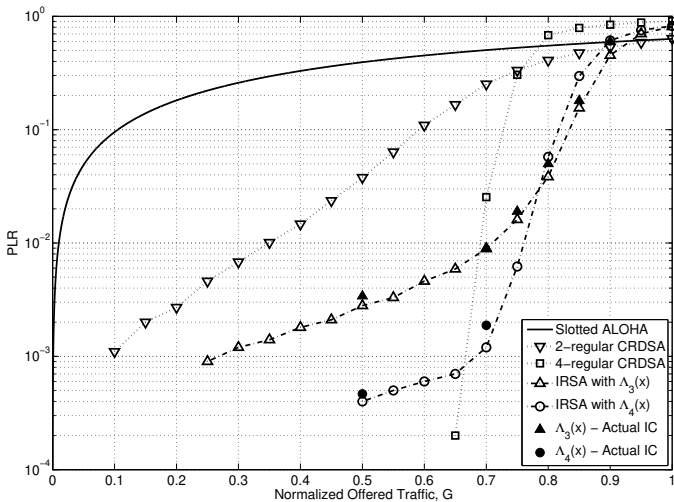


Fig. 7. Packet loss rates for SA, CRDSA with 2 and 4 repetitions, and for IRSA with $\Lambda_3(x) = 0.5x^2 + 0.28x^3 + 0.22x^8$ and $\Lambda_4(x) = 0.25x^2 + 0.60x^3 + 0.15x^8$, with $n=200$ and $I_{max} = 20$. The results obtained by simulating the actual IC mechanism (with 20 iterations) are denoted by the markers \blacktriangle and \blacklozenge for $\Lambda_3(x)$ and $\Lambda_4(x)$ respectively. $E_b/N_0 = 2$ dB.

Further results were obtained by simulating the entire IC process (details in the Appendix B). The bursts have been encoded via the (4096, 1992) concatenated extended Bose-Chaudhuri-Hochquenghem (BCH) - structured irregular repeat accumulate (S-IRA) code [30], [31] included in the last version of the DVB-RCS standard [4], [26], and transmitted with QPSK modulation. The throughput with actual IC and SNR at $E_b/N_0 = 2$ dB (being E_b the energy per information bit and N_0 the one-sided noise power spectral density) is depicted in Fig. 5. The results are provided for $G = 0.75, 0.8, 0.85$ and 0.9 . The throughput loss w.r.t. the MAC layer simulation case is inappreciable. In Fig. 7, the results obtained through simulation of the IC process are compared to those obtained through the MAC layer simulations for both

the $\Lambda_3(x)$ and $\Lambda_4(x)$ distributions. We collected results for $G = 0.5, 0.7, 0.75, 0.8, 0.85, 0.9$ in the $\Lambda_3(x)$ case, and for $G = 0.5, 0.7$ in the $\Lambda_4(x)$ case. The results at $E_b/N_0 = 2$ dB confirm what was observed before. The performance degradation with the actual IC algorithm is negligible in both the low and the high PLR regimes.

In Figure 8, the normalized efficiency is provided for the various schemes at different SNRs, for the case of $n = 200$ and $I_{max} = 50$. The overall received signal power has been fixed in a way that $E_s/N_0 = 0, 6, 12$ and 15 dB (with $E_s = E_b R_c \log_2 M$ being E_s the energy per symbol, R_c the channel coding rate and M the modulation order). The normalized efficiency of a scheme is then computed as the ratio between the capacity C_i (with $i = 1, 2, 3$ for SA, CRDSA with 2 replicas and IRSA based on $\Lambda_3(x)$ respectively) of the scheme under such received power constraint, and the capacity of the corresponding multiple access channel, C_{ref} [3]. The normalized efficiency of the schemes strongly depends on the SNR: at very low SNRs (e.g. 0 dB) SA shows better performance than both CRDSA/IRSA. At high SNRs, CRDSA and IRSA outperform SA, with an increasing gap in favor of IRSA as the SNR becomes higher. In between, there is a significant SNR range where CRDSA outperforms both SA and IRSA. Nevertheless, for many of the systems where SA is used (e.g., satellite systems) the actual limitation resides in the peak transmission power. In this case, the results to be considered for a performance comparison are those presented in Figs. 5, 6 and 7.

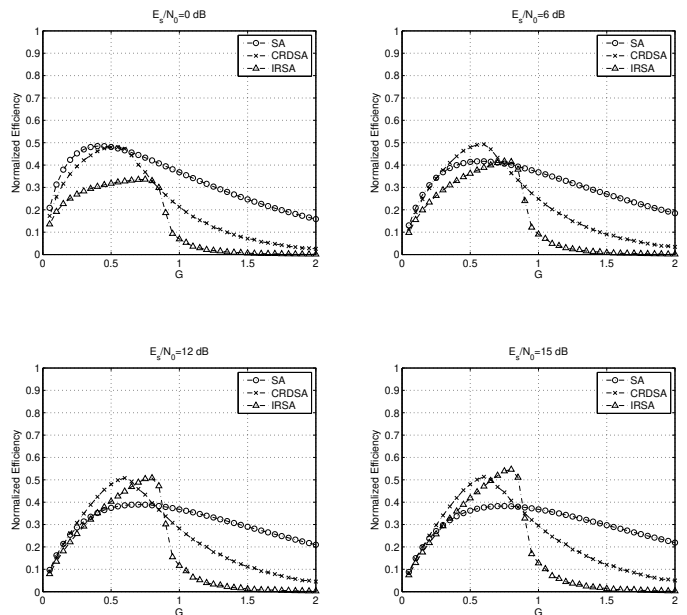


Fig. 8. Normalized efficiency for SA, CRDSA, and for IRSA with $\Lambda_3(x) = 0.5x^2 + 0.28x^3 + 0.22x^8$. Various E_s/N_0 values. $n = 200$.

VII. CONCLUSIONS

In this paper, an enhancement of the SA approach for MAC has been introduced. The proposed approach, named IRSA, represents an improvement of the CRDSA introduced in [9], allowing variable-rate burst repetition according to a

given probability distribution. The probability distribution is optimized by means of a novel bipartite graph representation of the IC process. Large gains in terms of throughput are achieved with respect to both conventional SA and CRDSA. It has been shown that IRSA is able to achieve a throughput close to $T \simeq 0.97$ in an asymptotic setting and near to $T \simeq 0.8$ in practical implementations, resulting in a throughput gain of $\sim 45\%$ with respect to CRDSA. An analysis in terms of normalized efficiency has been introduced, allowing comparisons under the assumption of equal average transmission power. Design criteria for the probability distribution are also introduced, which permit to achieve low floors for the packet loss rate. Simulation results, including an actual IC mechanism described in the Appendixes, substantiate the validity of the presented analysis and confirm the high efficiency of the proposed approach down to a signal-to-noise ratio as low as $E_b/N_0 = 2$ dB. The introduced graph representation constitutes a novel application of bipartite graphs to the analysis iterative receiver algorithms.

APPENDIX A

ANALYSIS IN PRESENCE OF IMPAIRMENTS AND CAPTURE EFFECT

The analysis developed in Section IV relies on the hypothesis that a burst can be recovered with probability 1 whenever the $l - 1$ bursts colliding in the same slot have been revealed. Nevertheless, the proposed analysis can be adapted to take into account more general conditions. To do so, let us first introduce the weights w_l , $l = 1 \dots \infty$, such that w_l represents the probability that a burst is successfully decoded after removing the interference contribution of the $l - 1$ colliding bursts [32]. We keep on denoting by $1 - q$ the probability that one among the $l - 1$ colliding bursts has been revealed elsewhere. It turns that the probability that the remaining burst is successfully decoded is

$$1 - p = w_l(1 - q)^{l-1}. \quad (8)$$

It follows that (2) can be rewritten as

$$p_i = \sum_l \rho_l \left(1 - w_l(1 - q_i)^{l-1}\right) = 1 - \tilde{\rho}(1 - q_i), \quad (9)$$

where $\tilde{\rho}(x) \triangleq \sum_l \rho_l w_l x^{l-1}$. Being from (5) $\rho(x) = \exp(-G\Lambda'(1)(1-x)) = \sum_l \rho_l x^{l-1}$, we thus derive the coefficients ρ_l of the Taylor series around $x_0 = 0$, resulting in

$$\rho_l = \frac{1}{(l-1)!} (G\Lambda'(1))^{l-1} e^{-G\Lambda'(1)}. \quad (10)$$

Recalling that $\rho(x) = \Psi(x)$ and that $\rho(x) = \sum_l \rho_l x^{l-1}$, $\Psi(x) = \sum_l \Psi_l x^l$, we have $\rho_l = \Psi_{l-1}$. It turns that (10) can be alternatively obtained by noting that for large n the number of collisions in a slot follows a Poisson distribution, $\Psi_l = (1/l!)(G\Lambda'(1))^l \exp(-G\Lambda'(1))$. The coefficients given by (10) can be used in (9) together with (1) to analyze the iterative IC process for a given choice of the probabilities $\{w_l\}$. As an example, one could analyze the case where $w_l = 1$ for $l \leq \bar{l}$, while $w_l = 0$ for $l > \bar{l}$. This setting represents the case where a non-linear effect (e.g. clipping,

saturation) jeopardizes the success of the IC process whenever too many collisions take place in a slot. In this case, $\tilde{\rho}(x)$ is the truncation of the Taylor series of $\rho(x)$ at the \bar{l} -th term, i.e.

$$\tilde{\rho}(x) = \sum_{l=1}^{\bar{l}} \rho_l x^{l-1} = e^{-G\Lambda'(1)} \sum_{l=1}^{\bar{l}} \frac{1}{(l-1)!} (xG\Lambda'(1))^{l-1}.$$

In a similar manner, an eventual capture effect can be taken into account in the analysis. To do so, it is sufficient to generalize the above-presented approach. We introduce the weight $w_{l,t}$, which denotes the probability that a burst replica can be decoded in a slot with l colliding packets, after removing t interference contributions. Considering a slot where l collisions took place, the probability to decode one burst is hence given by

$$1 - p = w_{l,l-1}(1 - q)^{l-1} + \sum_{t=0}^{l-2} w_{l,t} \binom{l-1}{t} (1 - q)^t q^{l-1-t},$$

where the term $w_{l,l-1}(1 - q)^{l-1}$ corresponds to (8) (case of no capture effect) and the term $\sum_{t=0}^{l-2} w_{l,t} \binom{l-1}{t} (1 - q)^t q^{l-1-t}$ accounts for the capture effect. By averaging over the BN distribution we finally get the modification of (9) as

$$p_i = 1 - \sum_l \rho_l \sum_{t=0}^{l-1} w_{l,t} \binom{l-1}{t} (1 - q_i)^t q_i^{l-1-t}. \quad (11)$$

APPENDIX B

IMPLEMENTATION OF THE IC MECHANISM

Let's consider the case where l users attempt a transmission within the same slot. We stick to the case of perfect power control and equal channel condition (gain) among the users. We denote by $u^{(i)}(t)$ the complex baseband pulse amplitude modulation (PAM) signal transmitted by the i -th user, i.e. $u^{(i)}(t) = \sum_{k=1}^{n_s} b_k^{(i)} \gamma(t - kT_s)$, where n_s is the number of symbols composing the burst, $\{b_k^{(i)}\}$ is the sequence of such symbols and T_s is the symbol period. By $\gamma(t) = \mathcal{F}^{-1} \left\{ \sqrt{CR(f)} \right\}$ we denote the pulse shape, being $CR(f)$ the frequency response of the raised-cosine filter.

Each contribution is received with a random delay ϵ_i , a random frequency offset $f_i \sim \mathcal{U}[-f_{max}, f_{max}]$ and a random phase offset $\phi_i \sim \mathcal{U}[0, 2\pi]$.¹⁵ The received signal after the matched filter (MF) is given by $r(t) = \sum_{i=0}^l z^{(i)}(t) * h(t) + n(t)$ where $n(t)$ is the Gaussian noise contribution, $h(t) = \gamma^*(-t)$ is the MF impulse response and $z^{(i)}(t) = \sum_{k=1}^{n_s} b_k^{(i)} \gamma(t - kT_s - \epsilon_i) \exp(j2\pi f_i t + j\phi_i)$. Assuming frequency shifts that are small w.r.t. the signal bandwidth (i.e., $f_{max}T_s \ll 1$), the received signal can be approximated by

$$r(t) \simeq \sum_{i=1}^l \tilde{u}^{(i)}(t - \epsilon_i) e^{j2\pi f_i t + j\phi_i} + n(t). \quad (12)$$

Here, $\tilde{u}^{(i)}(t)$ is the response of the MF to $u^{(i)}(t)$. We assume next that the contribution to be recovered is the one for $i = 1$, and the residual $l - 1$ contributions $\tilde{u}^{(2)}(t), \tilde{u}^{(3)}(t), \dots, \tilde{u}^{(l)}(t)$

¹⁵ $\mathcal{U}[a, b]$ denotes the uniform distribution over the closed interval $[a, b]$, while $\mathcal{U}(a, b)$ denotes the uniform distribution over the left-closed right-open interval $[a, b)$.

represent the interference to be cancelled. We consider moreover that the $l - 1$ interfering signals correspond to bursts that have been correctly decoded in other slots.

To proceed with the IC, it is necessary to estimate the set of parameters $\{\epsilon_i, f_i, \phi_i\}$, for $i = 2 \dots l$. As discussed in [9], we consider the case where ϵ_i and f_i can be accurately estimated on the corresponding burst replica that have been already recovered, and that their values remain constant through the frame. As pointed out in [9], this argument does not hold for the phase rotation terms ϕ_i , which may not be stable from a slot to another one. We need therefore to estimate ϕ_i for each burst directly on the slot where we want to eliminate its contribution. An estimator for ϕ_i is suggested in [9], which takes advantage of a training sequence included in each burst. A finer estimation can be obtained by a data aided (DA) approach. Recall in fact that the symbol sequences $\{b_k^{(i)}\}$ (for $i = 2 \dots l$) are known at the receiver, since they can be reconstructed from the twin packets decoded in other slots. The IC works as follows. We denote by $y^{(i)}(t)$ the signal at the input of the phase estimator for the i -th contribution. In the first step, the input signal is given by $y^{(2)}(t) = r(t)$ and the phase of the first interfering user ($i = 2$) is estimated as

$$\hat{\phi}_2 = \arg \left\{ \sum_{k=1}^{n_s} y_k^{(2)} \left(b_k^{(2)} \right)^* \right\}$$

with

$$y_k^{(2)} = y^{(2)}(kT_s + \epsilon_2) e^{-j2\pi f_2(kT_s + \epsilon_2)}.$$

After the estimation of the phase offset for the first interferer, the corresponding signal can be reconstructed as $\tilde{u}^{(2)}(t - \epsilon_2) e^{j2\pi f_2 t + j\hat{\phi}_2}$ and its contribution can be removed from (12), i.e.

$$y^{(3)}(t) = y^{(2)}(t) - \tilde{u}^{(2)}(t - \epsilon_2) e^{j2\pi f_2 t + j\hat{\phi}_2}.$$

The IC proceeds serially.¹⁶ For the generic i -th contribution,

$$\hat{\phi}_i = \arg \left\{ \sum_{k=1}^{n_s} y_k^{(i)} \left(b_k^{(i)} \right)^* \right\} \quad (13)$$

with $y_k^{(i)} = y^{(i)}(kT_s + \epsilon_i) \exp(-j2\pi f_i(kT_s + \epsilon_i))$ and

$$y^{(i)}(t) = y^{(i-1)}(t) - \tilde{u}^{(i-1)}(t - \epsilon_{i-1}) e^{j2\pi f_{i-1} t + j\hat{\phi}_{i-1}}.$$

After the cancellation of the $l - 1$ contributions, the residual signal will be denoted by $y^{(1)}(t)$ and is given by the 1-st user's contribution, the noise $n(t)$, and a residual interference term $\nu(t)$ due to the imperfect estimation of the interferers' phases (causing imperfect IC), i.e.

$$y^{(1)}(t) = \tilde{u}^{(1)}(t - \epsilon_1) e^{j2\pi f_1 t + j\hat{\phi}_1} + n(t) + \nu(t). \quad (14)$$

The estimation of $\{\epsilon_1, f_1, \phi_1\}$ is then performed on the signal of (14). After sampling, soft-demodulation takes place, and the log-likelihood ratios for the codeword bits are derived.¹⁷

¹⁶Due to the perfect power control, we proceed with the successive IC without any specific ordering of the users. In case of power unbalance, the IC may be enhanced by proceeding in the order of decreasing received powers [10]–[13].

¹⁷An accurate estimation of $\{\epsilon_1, f_1, \phi_1\}$ can be obtained by iterating decoding and estimation [33].

The advantage of this solution stems from the length of the sequence used for the phase estimation in (13). In [9] it was proposed to use a training sequence, which typically is few tens of symbols long. A burst can be composed by some hundreds (or thousands) symbols. This DA approach works if the cross-correlation between the sequences $\{b_k^{(i)}\}$, $i = 1 \dots d$, is on average low. This is indeed the case if each user encodes sequences whose bits $\{X_k\}$ can be modeled as independent and identically-distributed (i.i.d.) random variables, with $\Pr\{X_k = 0\} = \Pr\{X_k = 1\} = 1/2$. Alternatively, one may use for the estimation just the parity part of the codeword, which under certain conditions (e.g. the use of a channel code with good distance spectrum properties) presents sufficient randomness.

We simulated the IC process for slots with various numbers of collisions. The information sequences were randomly generated, then encoded through the (4096, 1992) code of the DVB-RCS standard [4], [26] which is obtained by the concatenation of an outer (2048, 1992) extended BCH code with an inner (4096, 2048) S-IRA code [30], [31]. QPSK modulation was considered for the simulations. It follows that each sequence $\{b_k^{(i)}\}$ is made by 2048 QPSK symbols. For each transmission attempt we generated the parameters $\{\epsilon_i, f_i, \phi_i\}$ according to the distributions presented before. The maximum frequency shift has been set such that $f_{max} T_s = 0.01$. The received signal $r(t)$ has been then oversampled at a rate M_s/T_s with $M_s = 8$, and the IC algorithm has been applied to the oversampled digital signal. Once the $l - 1$ interference contributions have been cancelled, log-likelihood ratios for the codeword bits have been input to the channel decoder. In Fig. 9 the impact of the IC process on the packet error rate (PER) for the burst to be recovered (i.e., the signal for $i = 1$) is shown in terms of PER vs. E_b/N_0 for $l = 2, 4, 8$ burst collisions. The performance on the additive white Gaussian noise (AWGN) channel without collisions is provided as reference. Note that, up to $l = 8$ collisions, the performance degradation due to the imperfect estimation of the phase offsets is small, i.e. less than 0.1 dB at $\text{PER} \simeq 10^{-3}$. Considering a SNR as $E_b/N_0 = 1.8$ dB, after removing $l - 1 = 7$ interference contributions we have $\text{PER} \simeq 10^{-3}$.

ACKNOWLEDGMENTS

The author would like to thank Matteo Berioli, Marco Chiani, Tomaso De Cola, Riccardo De Gaudenzi, Enrico Paolini and Sandro Scalise for their feedback on this work.

REFERENCES

- [1] N. Abramson, "The ALOHA system - another alternative for computer communications," in *Proc. 1970 Fall Joint Computer Conference*, vol. 37. AFIPS Press, 1970, pp. 281–285.
- [2] L. G. Roberts, "ALOHA packet systems with and without slots and capture," *ARPANET System Note 8 (NIC11290)*, June 1972.
- [3] N. Abramson, "The throughput of packet broadcasting channels," *IEEE Trans. Commun.*, vol. COM-25, no. 1, pp. 117–128, January 1977.
- [4] *Interaction channel for satellite distribution systems*, ETSI EN 301 790 v1.5.1, DVB Std., 2009.
- [5] D. Raychaudhuri and K. Joseph, "Channel access protocols for Ku-band VSAT networks: A comparative evaluation," *IEEE Commun. Mag.*, vol. 26, pp. 34–44, May 1998.

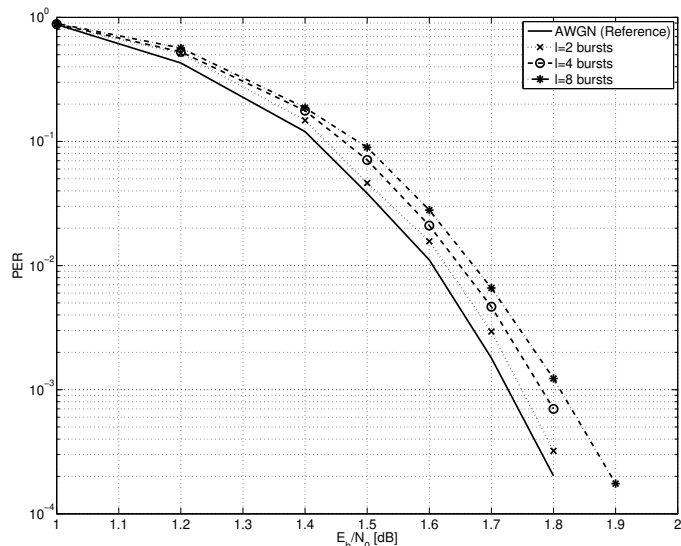


Fig. 9. PER vs. E_b/N_0 for the (4096, 992) S-IRA code of the DVB-RCS+M standard. QPSK modulation, 50 iterations of the belief propagation algorithm. Various number (l) of colliding packets.

[6] D. Raychaudhuri, "ALOHA with multipacket messages and ARQ-type retransmission protocols—throughput analysis," *IEEE Trans. Commun.*, vol. 32, no. 2, pp. 148–154, Feb. 1984.

[7] D. Bertsekas and R. G. Gallager, *Data Networks*. Upper Saddle River, NJ, USA: Prentice-Hall, Inc., 1987.

[8] G. L. Choudhury and S. S. Rappaport, "Diversity ALOHA - a random access scheme for satellite communications," *IEEE Trans. Commun.*, vol. 31, pp. 450–457, 1983.

[9] E. Casini, R. D. Gaudenzi, and O. del Rio Herrero, "Contention resolution diversity slotted ALOHA (CRDSA): An enhanced random access scheme for satellite access packet networks," *IEEE Trans. Wireless Commun.*, vol. 6, pp. 1408–1419, April 2007.

[10] T. M. Cover, *Some advances in broadcast channels*. San Francisco: Academic Press, 1975, vol. 4, chapter in the book "Advances in Communication Theory", edited by A.J.Viterbi.

[11] S. Verdú, *Multuser Detection*. Cambridge University Press, 1998, Chapter 7.

[12] A. J. Viterbi, "Very low rate convolutional codes for maximum theoretical performance of spread-spectrum multiple-access channels," *IEEE J. Sel. Areas Commun.*, vol. 8, pp. 641–649, May 1990.

[13] P. Patel and J. Holtzman, "Analysis of a simple successive interference cancellation scheme in a DS/CDMA system," *IEEE J. Sel. Areas Commun.*, vol. 12, pp. 796–807, June 1994.

[14] O. del Rio Herrero and R. D. Gaudenzi, "A high-performance MAC protocol for consumer broadband satellite systems," in *Proc. 27th AIAA*

International Communications Satellite Systems Conference (ICSSC), Edinburgh (UK), Jun 2009.

- [15] Next generation DVB-RCS standardization group. [Online]. Available: <http://www.dvb.org/technology/dvbrcs/>.
- [16] C. Morlet, A. B. Alamanac, G. Gallinaro, L. Erup, P. Takats, and A. Ginesi, "Introduction of mobility aspects for DVB-S2/RCS broadband systems," *IOS Space Communications*, vol. 21, no. 1-2, pp. 5–17, 2007.
- [17] R. Tanner, "A recursive approach to low complexity codes," *IEEE Trans. Inf. Theory*, vol. 27, pp. 533–547, Sept. 1981.
- [18] M. Luby, M. Mitzenmacher, and A. Shokrollahi, "Analysis of random processes via and-or tree evaluation," in *Proc. 9th Annual ACM-SIAM Symposium on Discrete Algorithms*, 1998, pp. 364–373.
- [19] M. Luby, M. Mitzenmacher, A. Shokrollahi, and D. A. Spielman, "Improved low-density parity-check codes using irregular graphs," *IEEE Trans. Inf. Theory*, vol. 47, no. 2, pp. 585–598, Feb. 2001.
- [20] T. J. Richardson, A. Shokrollahi, and R. L. Urbanke, "Design of capacity-approaching irregular low-density parity-check codes," *IEEE Trans. Inf. Theory*, vol. 47, no. 2, pp. 619–637, Feb. 2001.
- [21] R. G. Gallager, *Low-Density Parity-Check Codes*. Cambridge, MA: M.I.T. Press, 1963.
- [22] L. Kleinrock and S. Lam, "Packet switching in a multiaccess broadcast channel: Performance evaluation," *IEEE Trans. Commun.*, vol. 23, no. 4, pp. 410–423, 1975.
- [23] M. Luby, "LT codes," in *Proc. of the 43rd Annual IEEE Symposium on Foundations of Computer Science*, Vancouver, Canada, Nov. 2002, pp. 271–282.
- [24] R. Storm and K. Price, "Differential evolution - a simple and efficient heuristic for global optimization over continuous spaces," *Journal of Global Optimization*, vol. 11, no. 4, pp. 341–359, December 1997.
- [25] T. M. Cover and J. A. Thomas, *Elements of information theory*, 2nd ed. New York: Wiley, 2006, chapter 15.
- [26] G. Liva, M. Papaleo, C. Niebla, S. Scalise, S. Cioni, A. Vanelli-Coralli, G. E. Corazza, P. Kim, and H. J. Lee, "The very short frame of mobile DVB-RCS: Code design and QoS performance," *Int. Journal of Satellite Communications and Networking (Wiley)*, 2009, to appear.
- [27] C. Di, D. Proietti, T. Richardson, E. Telatar, and R. Urbanke, "Finite length analysis of low-density parity-check codes on the binary erasure channel," *IEEE Trans. Inf. Theory*, vol. 48, pp. 1570–1579, 2002.
- [28] A. Orłitsky, K. Viswanathan, and J. Zhang, "Stopping Set Distribution of LDPC Code Ensembles," *IEEE Trans. Inf. Theory*, vol. 51, no. 3, pp. 929–953, Mar. 2005.
- [29] M. Chiani and A. Ventura, "Design and performance evaluation of some high-rate irregular low-density parity-check codes," in *Proc. IEEE Globecom*, San Antonio, Texas, Nov. 2001, pp. 990–994.
- [30] Y. Zhang and W. E. Ryan, "Structured IRA codes: Performance analysis and construction," *IEEE Trans. Commun.*, vol. 55, pp. 837–844, May 2007.
- [31] W. E. Ryan and S. Lin, *Channel Codes – Classical and Modern*. Cambridge University Press, 2009.
- [32] G. Liva, "A Slotted ALOHA Scheme Based on Bipartite Graph Optimization," in *Proc. International ITG Conference on Source and Channel Coding*, Siegen (Germany), Jan 2010.
- [33] C. Herzet, N. Noels, V. Lottici, H. Wymeersch, M. Luise, M. Moeneclaey, and L. Vandendorpe, "Code-aided turbo synchronization," *Proc. IEEE*, vol. 95, no. 6, pp. 1255–1271, June 2007.